Towards a $\mathbf{2}\boldsymbol{D}$ model biopolymer polycrystalline aggregation based on Smoluchowski-type dynamics supplemented by computer experiment

N. Kruszewska, A. Gadomski

Department of Theoretical Physics, Institute of Mathematics and Physics,
University of Technology and Life Sciences,
Kaliskiego 7, Bydgoszcz PL–85796, Poland

(Received)

Based on a $2D$ version of the Smoluchowski-type model, formulated in a phase space of the linear objects' sizes R-s in terms of the mesoscopic nonequilibrium thermodynamics (MNET) as a guiding formalism/mechanism, we are looking in a comparative way for its basic trends and characteristics in a suitably designed Monte Carlo (MC) computer experiment on model biopolymer aggregation. The preliminary small-scale simulation results indicate that the examined hydrophobic-polar HP (dis)ordered aggregations bear two-type signatures of the underlying (complex) Smoluchowski dynamics. The first one is associated with a phase-separative tendency, showing up, in suitable conditions, lamellar ordering within the cluster, intermingled randomly with an amorphous phase. This is the case called by us the cylindrolite formation. The second-type signature, in turn, seems to point out some more disordered-from-within overall HP aggregations, presumably resulting in establishing a large HP mega-cluster, tending to span all over the available 2D simulation space. The quantitative characteristics derived so far show up at best an approximative tendency towards interpolating between this two types of aggregation/phase-separation signatures. A certain hope for better adjusting theory to computer simulation may come from realizing a non-Markovian character of the process which, for example, enables one to manipulate with the time scale in a case-sensitive, presumably excluded-area involving manner.

PACS numbers: 05.10.Gg, 05.10.Ln, 05.20.Dd, 05.60.Cd, 05.70.Ln, 05.70.Np, 61.46.+w

1. Introduction

The kinetic-thermodynamic behavior of biopolymer assemblages evolving under a two-dimensional shear-free confinement, occurring in soft materials, seems to be a very intriguing issue from both physical as well as

medical points of view. The observed microstructures are largely a result of some natural biopolymer folding and aggregation processes and can be represented as two-dimensional matter organizations [1, 2, 3]. A set of examples may include at least two representative cases. First, the formation of pathogenetic protein deposits in biological films, leading to neurodegenerative diseases such as Alzheimer, Parkinson, prion [4] or Creutzfeldt-Jakob diseases, or Renal Failure, is important for thorough exploration not only because of finding a cure on these diseases but also because of the fact that population of those disorders increases steadily over the years [5]. Second, based on Langmuir-Blodgett, or specifically Langmuir-Schaeffer technology, scientists are able to accelerate protein crystal growth which, in turn, enables to get at possibly low-cost valuable test samples needed by modern protein nanocrystallography [6].

In this paper, an attempt has been made to find out by means of the proposed Monte Carlo (MC) simulation some of the main trends of two-dimensional[1] aggregates' formation in model biopolymer matter (MBM) under semi-dilute (solution) conditions, and to compare them, if possible, with their known analytic counterparts originating from the Smoluchowski dynamics [10]. The MBM matter consists of HP chains: The HP chains are linear chains made of hydrophobic (H) and hydrophilic viz polar (P) residues [11]. Our approach is based on the possibly easiest although effective $2D$ lattice model called the tube HP (THP) model [12], utilizing a MC algorithm for computer simulations of polymer folding, extended as being applicable to the aggregation of HP chains, with an emphasis placed on proper folding conditions which favor a long-range (fibrillar) order within each model HP chain [12], and possibly, in clusters made of such chains [2].

From a molecular-level point of view, the MBM is readily mimicked by the HP chains, and preferentially, by their clusters. The folding and HP–chain clustering conditions are assured thanks to switching on the $H-H$ interaction mode of hydrophobic nature, while always disabling at the same time the other types of the interaction modes, like $P-P$ or $H-P$ ($P-H$). The effect of solution is generically built in the HP type description of MBM. The chains are subjected to a $2D$ confined movement which leads to numerous formations of the biopolymer clusters of versatile types, e.g. either polycrystals or disordered aggregates, distributed either sparsely (sol-like) or tightly (gel-like) all over available geometrical-physical space. Thus, when looking from supramolecular-level point of view, MBM

[1] A thorough motivation of exploring model biomatter aggregations exclusively in the (effectively) $2D$ space has been contained in [7, 8]. It mainly refers to a kinetic-thermodynamic optimality of such $2D$ evolutions occurring in viscoelastic [9] environments in which phase separation and sol-gel type phase changes take place under such geometrical confinement, e.g. the one due to adsorption.

is assumed to form by clusters which are made of a certain number of the HP chains connected by at least two $H-H$ interchain interactions. The clusters are always formed by sequences of folding - refolding events, wherein a refolding is attributed to aggregation of two or more HP chains. This is what both experiment and computer simulation are able to tell us [2]. From them both, however, one is also able to get some typical cluster - cluster aggregation (CCA) characteristics [13]. As examples, one may invoke here: (i) an average number of clusters involved in the CCA; (ii) an average radius, characterizing a CCA under examination; (iii) an average area covered by CCA; etc. These are also the observables characteristic of some percolation system such as the one prone to gelation [7, 8, 13]. Fortunately, all characteristics, (i)÷(iii), etc., are also fairly accessible by Smoluchowski-type dynamics [14, 15], in our approach applied in terms of a (discretized) mesoscopic nonequilibrium thermodynamics (MNET) system [14], working preferentially in the space of the cluster sizes[2]. In this way, we allow ourselves to take an opportunity to compare this type of well-known (Smoluchowski) theory [8, 15] with the results obtained from our computer simulation of the biopolymer CCA.

The goal of this paper is to get some preliminary dynamic characteristics of our MC-based CCA, resulting from HP-chain interactions of $H-H$ type, revealing the characteristics (i)÷(iii) mentioned above, and to compare them thoroughly, whenever possible, to their mainly analytic counterparts, coming from the Smoluchowski approach [15, 16, 17]. We present a preliminary but quite systematic study on the growing stage, also emphasizing here (a) the statistical distributions of non-Gaussian (Weibull) character; (b) sol-gel type tendencies [16] towards the phase changes due to suitable alterations of the ratio

$$\delta_{HP} = \frac{\#H}{(\#H + \#P)}, \tag{1}$$

pointing to the relative number of the H groups in the (average) cluster; here the symbol # denotes the number of H and P residues in the chain, respectively.

The purpose of such exploration is to find out in which kinetic-thermodynamic conditions microstructures such as $2D$ micelles (HP aggregates) or fibrils-involving polycrystals called the cylindrolites may appear [17]. In order to do so, let us realize that, one of the most important parameters for this model is also the concentration, which is defined as a relative number of

[2] In the position space of the centers of mass of the clusters we rather encounter a diffusion-reaction problem, with a chemical reaction source coming from $H-H$ interactions; there is no explicit drift term available therein, resulting mainly from the free energy changes, presumably over some respective changes of clusters' radii [10].

monomers included in the space over which the HP chains are distributed. (So far, however, we present some results for fixed concentration values of $\rho = \frac{1}{10}$ or $\rho = \frac{2}{5}$.) Moreover, it turns out that the cluster size and shape appear to be a result of presence of the hydrophobic residues in HP chain, thus of the ratio δ_{HP} as a consequence thereof, cf. Eq (1). The ratio δ_{HP}, in turn, when being considered as a global measure, extended to the HP clusters, constituting the MBM, depends on the concentration ρ.

In next two sections, we discuss dynamic parameters of the aggregations looking at them from molecular and supramolecular points of view, Sections 2 and 3, respectively. In Section 4, we present and discuss some first results obtained from the computer simulation, and how do they conform, or do not conform, to those available from Smoluchowski (MNET) framework [7, 8, 10, 18]. Our efforts will be summarized in the concluding address and perspective (Section 5), where a certain way of how to try to comprehend the obtained computer-simulation results just in terms of their analytic counterparts, regarding a pivotal role of time scale and non-Markovianity in the Smoluchowski framework [10], has been suggested.

2. Microscopic HP chain dynamics as manifested at a molecular and few-clusters levels of description

Biopolymer chains immersed in an aggregating milieu striving for the lowest possible energy, undergo the folding process disturbed consequently by some assisting aggregation acts. The first step of our simulation is to generate biopolymer chains using self-avoiding random walk algorithm, and in subsequent steps, allow them to fold using MC algorithm [11, 12, 19]. In our obstructed version of the $2D$ Go-type model [20], $H-H$ contacts are in favor and they are selected in a temperature-dependent way[3] by means of a dimensionless energetic parameter ($H-P/P-H$ and $P-P$ contacts do not influence formally the process), namely

$$\Delta\varepsilon = \frac{\Delta E_{H-H}}{k_B T} \tag{2}$$

(k_B - the Boltzmann constant). As argued by others [11], in the HP model $\Delta E_{H-H} = -1[k_B T]$ can be assumed (and for THP $\Delta E_{H-H} = -3 \div -1[k_B T]$ [12]), and has also been taken in our simulations. By manipulating $\Delta\varepsilon$ we can control over the free energy $\Delta\Phi$ to be specified more accurately in the next section.

Note only right here, that because the control should be consistent with the analytic Smoluchowski framework [11], we are going to keep track of

[3] Under a temperature value, T, typical for the room-temperature experiment that we actually describe [2].

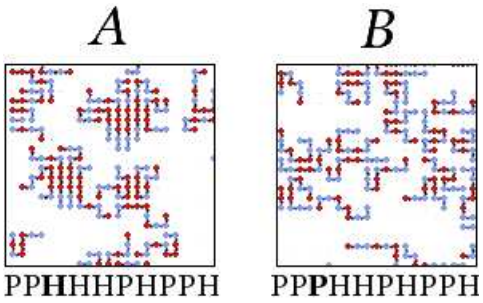

Fig. 1. Example of (non)crystallized hydrophobic cores (dark dots) with their hydrophilic borders (light dots) depending upon the δ_{HP} ratio (for a given T): (A) $\delta_{HP} = \frac{1}{2}$, a tendency for obtaining a long-range order within each $2D$ discrete object viz cylindrolite [17] is observed; (B) $\delta_{HP} = \frac{2}{5}$, some different tendency of creating $2D$ discrete objects with non long-range order prevails. A small local change in favor of hydrophobicity (changing one P residue over one H residue in the chain sequence, cf. slightly different HP sequences of $n_{HP} = 10$ length chains, characteristic of some bold-faced H to P single replacement - look at the bottoms of both parts A and B of the plot) causes a quite drastic global change in the overall HP structure. (Presented are three-day simulation results based on THP model with $\rho = \frac{2}{5}$.)

$-\frac{\Delta\Phi}{k_BT} \propto R$ [7, 8] for globally undense ("high-temperature") and $-\frac{\Delta\Phi}{k_BT} \propto lnR$ [10] for globally dense ("low-temperature") HP aggregates, respectively, formed at the supramolecular level, in order to see whether such a tendency, derived analytically [7], is to be present in our MC simulation. In the THP model, energy ΔE_{H-H} is dependent upon an overall amount of rearranging monomers before and after the native contacts are established. This THP model prefers parallel configurations and is aimed to obtain some readily crystallized macrostructures [12], cf. Fig. 1. Note, however, that such a propensity to crystallization, offered naturally by the THP model, would ultimately remain inapplicable to form (poly)crystals as far as an insufficient number of H residues spoiled the long-range ordering in its fibrillar (lamellar) form, see Fig. 1. On the contrary, preferring $H-H$ contacts leads typically, for a suitable range of T (temperature) values, to obtain a cluster's body consisting of a crystallized hydrophobic core with some hydrophilic border embracing it, wherein the structure of the border can be quite fuzzy or hairy viz irregular, cf. Fig 2, though sometimes with appreciably small aspect ratio. This is to say that such clusters can also be of nearly round shape, characteristic of biopolymer cylindrolites [17].

3. Mesoscopic HP chain clusters' dynamics as revealed at a supramolecular (many-clusters) level of description

The $2D$ matter evolutions of interest undergo, in general, the following scheme which relies on having three stages of the evolution being involved: (i) nucleation stage; (ii) growing stage (GS); (iii) cessation-to-growth (termination) stage. First, since our computer simulations suffer from a finite-size effect (they are small-scale simulations so far) we did not explore stage (iii) which demands a truly long-time scale [8]. Second, we have attempted to explore stage (i). From our preliminary considerations, it follows that under the notion of stable (viz, non-disappearing) nucleus, we may understand such an "heavy" outcome that experiences possibly small changes in its translational motion. It implies that we assign rather a kinetic (non-classical) than thermodynamic meaning to the nucleation stage [16, 21], not postponing totally the latter, however. Third, throughout the paper's body we extensively explore the GS in terms of its most interesting tendencies because it is the only stage witnessing truly a non-equilibrium MNET-oriented character of the process. It suits very well the conception of the Smoluchowski framework which we take as a reference to our simulations [15, 16]. A few aggregations are presented in Figs 2 and 3.

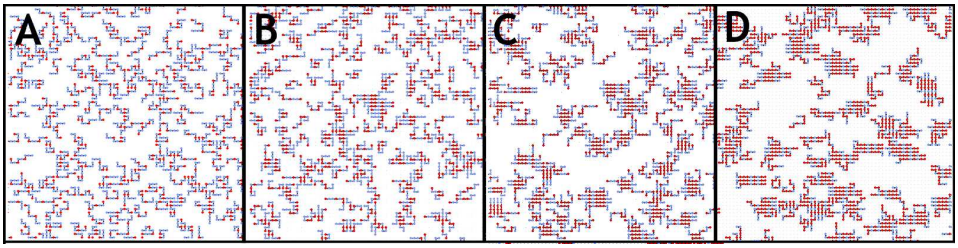

Fig. 2. Four THP microstructures with $\rho = \frac{2}{5}$, and a standard set of ΔE_{H-H}-s taken from the THP model [12], are presented upon certain δ_{HP} changes, indicating at first glance a sol-gel tendency manifested while decreasing δ_{HP} value from right to left: (A) $\delta_{HP} = \frac{3}{10}$; (B) $\delta_{HP} = \frac{4}{10}$; (C) $\delta_{HP} = \frac{5}{10}$; (D) $\delta_{HP} = \frac{6}{10}$. Realize that the bigger δ_{HP} is the larger the voids are left amongst the HP clusters, although the more ordered the clusters can be (the role of δ_{HP} as an order parameter may arise). Such a picture, especially Figs 2C-D, fairly resembles an effect of (viscoelastic) phase separation of (poly)crystalline phase which manifests in close touch to sol-gel phase change, not achieved yet [7, 9]; also notice that, the mean degree of crystallinity for clusters, quantified by an account of the lamellar phase in the system, is changing with an increase of δ_{HP} value, and approximately equals to (A) $\frac{5}{100}$, (B) $\frac{16}{100}$, (C) $\frac{19}{100}$ and (D) $\frac{33}{100}$, respectively (quite a big jump between $\delta_{HP} = \frac{5}{10}$ and $\delta_{HP} = \frac{6}{10}$ can be noticed).

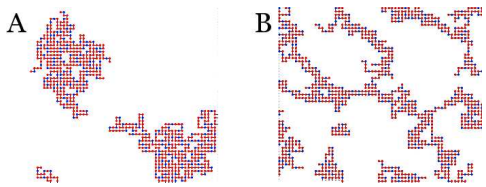

Fig. 3. A comparison of two distinctly different microstructures, obtained during low-density (small ρ) computer simulations: (A) closely packed from within ($\Delta E_{H-H(intrachain)} = -1[k_BT]$); (B) loosely packed from within ($\Delta E_{H-H(intrachain)} = -0.5[k_BT]$) - some nuclei of a network (gel-like) microstructures can be seen, with a clear tendency to elongation, which is an elastic property. Both these simulation results point to the same parameters $\rho = \frac{1}{10}$ and $\delta_{HP} = \frac{3}{4}$. In the simulation, we distinguish between inter- and intrachain interaction $\Delta E_{H-H(intrachain)} = \frac{2}{3}\Delta E_{H-H(interchain)}$, applied to (A) and (B), respectively.

The Smoluchowski framework and its continuous as well as discretized versions have been presented below in a sketchy way - an interested reader is encouraged to consult [10, 17].

In this section, we would like to present the $2D$ polycrystal growth model as driven by the rate of entropy change in our biomolecular dispersive-drifter (binary system), manifesting typical MNET properties [14].

One of the MNET primary assumptions is a positive entropy production in the system. As for our system, when temperature is kept constant over time, the entropy production equation comes directly from 1st law of thermodynamics[4]

$$TdS = -\mu dM, \tag{3}$$

where S, μ and M have their usual meaning [18]. Eq. (3) via the flux-force $J = \sum_j^2 L_{ij}X_j$ ($j = 1, 2$) (L_{ij} stand for the Onsager's coefficient while X_j represent both thermodynamic forces of diffusive and drifted nature) relations, and the continuity equation [18]

$$\frac{\partial P(R,t)}{\partial t} = -\frac{\partial J(R,t)}{\partial R}, \tag{4}$$

where $P(R,t)$ stands for the probability distribution of finding the HP cluster (the best option: the cylindrolite) [17] of linear size R at a given instant t, after rewriting $J(R,t) = -D(R,t)\frac{\partial P(R,t)}{\partial R} - B(R,t)\frac{\partial \Delta\Phi}{\partial R}P(R,t)$,

[4] Our system is an entropic system, i.e. $T\Delta S \gg \Delta H$, in which the entropy is supposed to create some interesting order (towards cylindrolites [17]) vs disorder (towards aggregates [13]) effects.

gives ultimately the Fokker-Planck-Smoluchowski (F-P&S) equation [8, 15]

$$\frac{\partial P(R,t)}{\partial t} = \frac{\partial}{\partial R}\left(D(R,t)\frac{\partial P(R,t)}{\partial R} + B(R,t)\frac{\partial \Delta\Phi}{\partial R}P(R,t)\right), \qquad (5)$$

where the mobility $B(R,t) = \frac{D(R,t)}{k_B T}$ ($D(R,t)$ is the diffusivity of the cluster formations) in the R-space, with the free energy $\Delta\Phi$ included in the formalism, see the preceding Section. In order to compare effectively the Smoluchowski-type model with the result of our computer experiment let us also write down a discrete version of equation (4) or (5)

$$P(R,t+\Delta t) = P(R,t) - \frac{1}{v_{jump}}\left(J(R+\Delta R,t) - J(R,t)\right), \qquad (6)$$

where $v_{jump} = \frac{\Delta R}{\Delta t}$, and the flux reads

$$\begin{aligned} J(R,t) = \quad & -D(R,t)\frac{P(R+\Delta R,t) - P(R,t)}{\Delta R} \\ & -\frac{1}{k_B T}D(R,t)\frac{\Delta\Phi(R+\Delta R) - \Delta\Phi(R)}{\Delta R}P(R,t), \end{aligned} \qquad (7)$$

$$\begin{aligned} J(R+\Delta R,t) = -D(R+\Delta R,t)\frac{P(R+2\Delta R,t) - P(R+\Delta R,t)}{\Delta R} \\ -\frac{1}{k_B T}D(R+\Delta R,t)\frac{\Delta\Phi(R+2\Delta R) - \Delta\Phi(R+\Delta R)}{\Delta R}P(R+\Delta R,t). \end{aligned} \qquad (8)$$

Initial and boundary conditions obey

$$P(R,t) = P(R+\Delta R,t) = 0, \qquad (9)$$

or equivalently (in a MNET-like manner [18], cf. Eqs (6)-(9))

$$J(R,t) = J(R+\Delta R,t) = 0, \qquad (10)$$

and

$$P(R+2\Delta R, t=t_0) = P_0, \qquad (11)$$

can freely be chosen as an initial (input) value. Eqs (6)$\div$(11) represent a (virtually) working scheme which we did not apply explicitly to our simulation yet although they: (A) conform well to the discrete character of our process; (B) help in understanding the obtained evolutions; for example, from them it is seen that the MNET BCs (Eq. (10)) are fulfilled and that the free energy (change) $\Delta\Phi$ subjected to a change in-linear size

ΔR, appears to be really the main driver of the examined process, cf. Eqs (7)÷(8). (Note that the scheme (6)÷(11) stated above is exclusively the explicit finite-difference scheme with its characteristic R- and t-increments in discrete size- and time domains, ΔR and Δt, respectively.) Since, for a given time t, the solutions to the F-P&S equations are known and take typically the form of the Weibull function $f(x|a,b)$, to be presented in a general form as [17, 22]

$$f(x|a,b) = ba^{-b}x^{b-1}e^{-\left(\frac{x}{a}\right)^b}, \tag{12}$$

($x > 0$ - arbitrary argument; a, b - fitting parameters), we then use this function for fitting our simulation data, cf. Fig. 4. It is in a fair agreement with what we get analytically [10, 17], wherein the obtained $P(R,t)$-s conform appreciably to the general mathematical (fitting) form presented by Eq. (12). The presented statistics, can be directly related with the elementary definition of $P(R,t)$, given by $P(R,t)dR = dn(R,t)$ [8, 10] which points to the number $dn(R,t)$ of clusters of a size taken from $[R, R+dR]$, this way enabling to relate ultimately the probability $P(R,t)$, deal with as a number density, with an occurrence of the cluster of a given size, as depicted in Fig. 4.

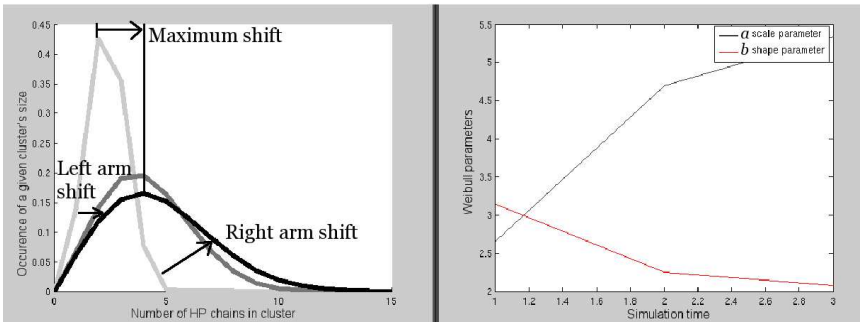

Fig. 4. Weibull-fitted histogram (Eq. (12)): the number of clusters as a function of the attained size in the beginning (light line), in-between (gray line) and in the end (dark line) of the three-day ($t_s = 3$ days) simulation of HP aggregation the population of which consists of 400 chains (left); on the right-hand side some controllable variations of the fitting parameters a and b have been depicted.

4. Results and discussion

The preliminary small-scale simulation results obtained indicate that the examined hydrophobic-polar HP (dis)ordered aggregations bear two-type

signatures of the underlying (complex) Smoluchowski dynamics. The first-type signature is associated with a phase-separative tendency, manifesting in such a model viscoelastic HP medium, favoring, however, when starting from a given, suitably large, relative number of H residues in an average cluster, lamellar ordering within the cluster. This is the case called by us the cylindrolite formation [17]. The second-type signature, in turn, achievable for small-to-moderate values of the relative number seems to point to some more disordered-from-within [13] overall HP aggregations, presumably resulting in establishing a large HP mega-cluster, spanning (almost) all over the available $2D$ simulation space, herein the square lattice. Thus, the quantitative characteristics derived so far, especially Figs 5-7 below, show up at best an approximative tendency towards interpolating between the two types of aggregation signatures also known as the Smoluchowski dynamics in the phase space of the cluster sizes [16, 17, 19].

The major MNET-type tendency observed is revealed by the presence of the Weibull-type asymmetric cluster-size distributions [22] (see Eq. (7) therein) characteristic of the examined MBM organizations, cf. [16, 17] and refs. therein, as well as look at Fig. 4. One can see two significant changes in cluster size distributions in each presented time step. They can be attributed to the asymmetry of the distributions. They point to: (i) maximum shift towards bigger cluster sizes; (ii) a difference between lifting and dropping tendencies of the left and right arms of the distribution, respectively, cf. Fig. 4. The property (ii) points out the experimentally proven observation that smaller clusters always disappear at the cost of their bigger (neighboring) counterparts, which is also a principal landmark of the Smoluchowski dynamics we have in mind [7, 8, 13, 17].

The three presented characteristics (Figs 5-7), based on the simulation result, showing type of aggregation presented by Fig. 2(D), and some careful inspection of the picturesque tendencies seen from Figs 2 and 3 enable to conjecture that our $2D$ HP aggregations are specific able to undergo a passage between the sparsely distributed sol and network-like states, and may indicate which aggregation form (loosely- or closely-packed; scattered, lamellar or crystalline) we are eventually dealing with. From [16] it clearly follows that there is a correspondence between percolation-type evolutions and their MNET counterparts, at least from the kinetic point of view. It should be pointed out that both characteristics $n(t)$ (Fig. 5) and $r(t)$ (Fig. 6) require quite an advanced derivation within the analytic Smoluchowski framework [7, 8, 10, 16, 17] whereas their derivation while based on the computer simulation is relatively simple [21].

In Fig. 5, we present the number of clusters n as a function of the simulation time t_s. For cylindrolites the number of ordered clusters, $n(t) \propto t^{-\frac{7}{6}}$ [17]; the same quantity for aggregates $n(t) \propto t^{-\frac{2}{3}}$ [22]. From our estima-

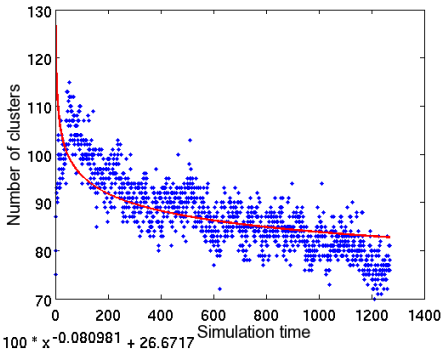

Fig. 5. The number of clusters n as a function of the simulation time t_s. The fitting function is presented at the bottom of the figure. Note, however, that the fitted data tend to slightly change the course at about $t_s = 1150$, which might indicate a still non-late stage of the process.

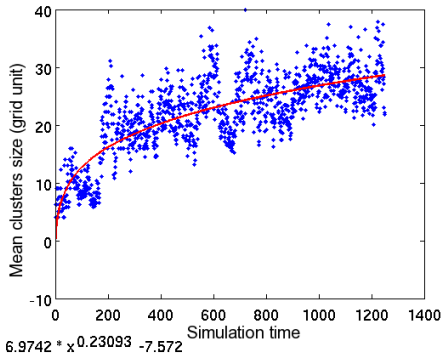

Fig. 6. An average cluster size r as a function of the simulation time t_s. The fitting function is presented at the bottom of the figure.

tion, seen at the bottom of Fig. 5, it appears that $n(t) \propto t^{-\frac{2}{25}}$, thus there appears some discrepancy between simulation and MNET characteristics. We will try to explain it later. In Fig. 6, an average cluster size r as a function of the simulation time t_s is presented. For (dis)ordered aggregates long-time results coming from continuous version of MNET [14] look like: (i) for cylindrolites $r(t) \propto t^1$ (a nearly constant-tempo growth) [23], (ii) for other aggregates $r(t) \propto t^{\frac{1}{3}}$ (a phase-separation, decreasing-in-time characteristics [16]). Our estimation, see the bottom of Fig. 6, yields so far $r(t) \propto t^{\frac{1}{4}}$, thus quite close to the phase-separation characteristics but still,

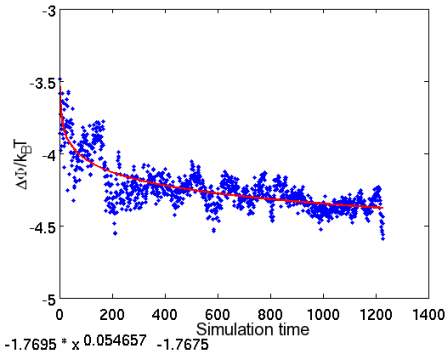

Fig. 7. The free energy value $\frac{\Delta\Phi}{k_BT}$ as a function of the simulation time t_s. The fitting function is presented at the bottom of the figure.

as in Fig. 5, some discrepancy between simulation and MNET results can be mentioned here. Notice, that in both characteristics the overall course of changes agrees only qualitatively with its analytic counterpart, derived as long-time asymptotics [8, 10, 17].

In Fig. 7, the free energy $\frac{\Delta\Phi}{k_BT}$ is shown as a function of the simulation time t_s. This free energy is obtained using $-\Delta\Phi \simeq ln[S(t)]$, where $S(t)$ is the area within a circle of the radius $r(t)$ (this radius is averaged over all aggregates appearing in time t). For cylindrolites $-\frac{\Delta\Phi}{k_BT} \propto ln\left(\frac{R}{R_0}\right)$ [10, 17], for aggregates $-\frac{\Delta\Phi}{k_BT} \propto \frac{R}{R_0}$ along with $R \propto t$ and $R \propto t^{\frac{1}{3}}$, respectively, where R-s should go quite in tact (in time) with R-s, specified by their time-scaling formulae above. Introducing the exponent's value from the approximation presented in Fig. 6 ($r \propto t^{\frac{1}{4}}$) to the free energy fitting function $-\frac{\Delta\Phi}{k_BT} \propto t^{\frac{1}{20}}$ one obtains a dependence of $-\frac{\Delta\Phi}{k_BT} \propto r^{\frac{1}{5}}$. At this point, by accepting the above logarithmic formula [10], we suggest that the obtained structure will be closely-packed (dense). Therefore, both cases, a colloid-type aggregations with loosely distributed clusters [7, 8] and a closely-packed polycrystalline aggregations [17], amongst a few characteristics, differ also when looking at their free energies, $\Delta\Phi$. In the former, a linear-in-R case has basically been derived [8], although when considering a fractal character of the cluster (Figs 2-3), it can be rewritten [7] as a power-like nonlinear relation $\Delta\Phi \propto \left(\frac{R}{R_0}\right)^{\frac{d_f}{2}}$, where typically $d_f = 1.6$ (but it can go towards lower values as well), see Fig. 7. In the latter, in turn, $\Delta\Phi$ goes like $\Delta\Phi \propto ln\frac{R}{R_0}$ (supported somehow by $R \propto t$), since in the close-packing limit the cylindrolites are approximated by

the circles with $d_f = 2$, thus, contrary to the above, giving no ample space for (colloidal or HP) fractality to enter. Moreover, this type of ordered structure emerges from the solution due to a phase separation, and because of the inherently non-negligible role of the solvent (H_2O), presumably due to a viscoelastic (spanning) effect [9]. Internal ordering, in turn, does not favor a total spanning over the lattice, which is only amenable when a not-so-high value of H residues comes into play, see Figs 2-3.

From our simulation data it follows that the aggregations go much slower than in loosely- or closely-packed case obtained analytically in the long-time limit [7, 8, 17]. The main cause of such a discrepancy relies practically on two observations: the possibility of HP chains detachment included in MC model (but not included in the MNET-type picture) and small-time and small-size scale simulations performed. Short chains have quite a big possibility to "walk" on the lattice, thus a big freedom of movement. Because of having small clusters involved, the probability of detachment for any HP chain to be finally connected to another HP chain by a single connection lies within $e^{-3} \div e^{-1}$, depending on a type of connection. Thus, a relatively big number of detachment events in small clusters is the main obstacle, whereas for bigger clusters this effect is negligible because of trapping the chains inside the cluster. As for the close-packing [8] as a whole, in all cases mentioned, and shown in Fig. 2, one can always observe voids between clusters, either relatively small or just large. But the voids preserve over all MC simulation, so that we may rather speak of loosely-packed structures than of some readily closely-packed.

5. Concluding address and perspective

To conclude, we have a monodispersive distribution of equal-length HP chains that can (i) move randomly; (ii) fold; (iii) and finally, aggregate, forming either more ordered clusters, termed by us cylindrolites, that may resemble the Eden flocks [24] or melted $2D$ Wigner quasi-crystals [1], or more disordered aggregates that are sometimes able to span over quite a large subspace of the available space. They can also be seen as quite elongated, presumably due to activated microrheological effects arising because of typically asymmetric $H - H$ contact distributions in the overall MBM so defined [25], assisted by some excluded-area effect [19]. These effects can be attributed to some viscoelastic phase separation occurring in the $2D$ amphiphilic system that we actually examine, cf. [9] and Figs 2 and 3 of Sec. 3.

Moreover, a carefully corroborated phase diagram, with the order parameter δ_{HP} examined in the course of the HP molecules' concentration, at some given T values, can certainly enlighten some peculiarities of the

studied process even more, cf. Ref. [2] and the phase diagram available therein.

Phenomena, and characteristic behaviors of similar type to these presented in this work can also be found in other systems, such as ferro- vs paramagnetic or (wet, force-free and prone-to-elongation) granular [26, 27].

To sum up in part, as some, either shortages or non-MNET including parts of the presented modeling, one may see the following:

- small-scale simulations have exclusively been applied so far (typically, the simulation matrix is $L \times L$, where $L = 100$ and the length of a HP-molecule $l_{HP} = 10$);
- simulation "time" t_s is clearly not a real time[5], so that we have so far no special feeling about the stationary (long-time) states, if exist, and the CtG effect (to appear in finite-size configurations) [28];
- molecular nature enters in its simplified HP form the computer model and is, unfortunately, not included at all in any MNET description [10, 11];
- no polydispersion of the HP-chain length, pointing towards more realistic description of the aggregations, has been involved so far;
- possibility of random detachment is present generically in the model but is totally absent in MNET-type description of the aggregations [10, 16] to which we compare our simulation results.

The above mentioned constitute the main course of as-yet immature configurations obtained that show up unquestionably a MNET-oriented tendency but in a (so far) qualitatively approaching way, cf. Figs 5-7. To remedy this, it should not be likely permitted to compare the simulation data directly to the analytic results too tightly but rather to continue the approach with its properly discretized version, see Eqs (6)-(11). In particular, a proper adjustment of the time scale, coming directly from our analytic considerations [10, 17] can be proposed, thus leaving the problem with an appropriate (fractal-like) form of $D(R,t)$ involved in Eq. (5). As is known [22], at least an asymptotic form of $D(R,t)$ can be proposed as $D(R,t) \propto \frac{R^{\alpha_1}}{t^{\alpha_2}}$ (for $t >> t_0$), where α_1 is a known mainly geometrical exponent [10, 17] whereas α_2 can be thought as some suitably adjusting and case-sensitive parameter. Such an inverse power-law type relation in time (t) comes from the physical fact that we typically deal with a non-Markovian process [25, 27] in which the viscosity of MBM changes due to inhomogeneities coming from the (non)linear excluded-area effect [19] clearly seen from Figs 1-3.

[5] A properly rescaled time has to be included inevitably in our future simulation tasks.

Moreover, let us remark that in our model we have implicitly included H_2O. By definition, a rule applies that the H residue does not like water whereas the P residue of any HP biomolecule does - an extension of the above can then be seen towards explicit involvement of H_2O [29].

Next, let us repeat that the preliminary small-scale simulation results obtained indicate that the examined hydrophobic-polar HP (dis)ordered aggregations bear two-type signatures of the underlying (complex) Smoluchowski dynamics: a phase-separative tendency [9], and predisposition to establishing a large HP mega-cluster [8], spanning all over the $2D$ simulation space, thus interpolating somehow between these two types of aggregation/phase-separation signatures. An open question remains, as for completing suitably the Smoluchowski framework in order to accomplish a better approximation to the MC simulation data, cf. the time-scale considerations toward a refinement [10, 17, 22].

Thus, as for the perspective, let us underscore that the scaling formula such as $r^2(t) \propto t^{2/(d+1)}$ [16], whereby $d = 2$ with the rescaled time $t \to t^{\alpha_2}$ can effectively be used to get the particle mean square displacement (*msd*) of specific semi-concentrated colloid-type HP systems. (Notice that α_2 has to be a truly fitting parameter/exponent, uncovering some merely viscous properties of the specific HP aggregation of interest.) For instance, in the case of the sol-gel continuous phase transition reported in [30] the exponent of the initial and final phases can be acceptably well-reproduced by taking into account the dominant role of clusters' surfaces (lines, in a $2D$ space) [16], as was also applied in [7, 8].

In our nonequilibrium-thermodynamics model [10, 17], the characteristic (geometric) exponent $\chi = 2/(d+1)$ of these phases corresponds to $\chi = 1$ for $d = 1$ (no surface) and $\chi \approx 0.66$ for $d = 2$ (a planar geometry) which is very close to a measured value of 0.7, see Figure 4 of Ref. [30]. Thereby, experiment and theory reveal almost the same exponents' values under which the same dynamic behavior, i.e. a passage from a diffusive (sol) to some subdiffusive (gel) state can be seen [7, 8]. This is also confirmed by relaxation measurements, cf. Figure 3 of the mentioned paper [30] and our considerations offered below.

The *msd* stated ultimately here by $r^2(t) \propto t^{2\alpha_2/3}$ [16] can be further related with the so-called creep compliance $\kappa(t)$ (a mechanical property), defined by the average strain to be assigned to a probe particle an HP cluster, immersed in our HP viscoelastic medium, divided by the corresponding shear stress [30], namely $r^2(t) \simeq \kappa(t)$. (Certainly, the strain always arises from asymmetric distributions of $H - H$ contacts.)

In the microrheological high-T milieu considered in Refs. [7, 8], we have made an attempt to define the inverse of $\kappa(t)$, namely $\kappa^{-1}(t)$, as the internal matrix stress $\sigma_M(t)$ accumulated within the inter-cluster spaces of

the matrix, assuming that in the late-stage growing conditions the average strain can approach a constant.

Thus, the viscoelastic properties of the HP aggregations can also be analyzed by means of their *msd*-involving behavior, provided that (i) one readily enters the late-time zone; (ii) the effectively $2D$ space is a space optimal from thermo-kinetic point of view [7, 8]. In view of the above, our HP aggregations manifest a really slowly creeping behavior, cf. Figs 5 and 6 for details.

Acknowledgements

The authors wish to thank prof. M. Cieplak IF PAN Warsaw for pointing out Refs [2] and [12]. (Un)folding-and-aggregation aspects based on model biopolymers are subject to a KBN grant 2P03B 03225(2003-2006) regulations. A.G. acknowledges a support by the ESF Programme Stochastic Dynamics: Fundamentals and Applications (STOCHDYN 2007).

REFERENCES

[1] X.H. Zheng, J.C. Earnshaw, *Europhys. Lett.* **41**, 635 (1998).

[2] R.I. Dima, D. Thirumalai, *Protein Sci.* **11**, 1036 (2002).

[3] A. Ulman, *Chem. Rev.* **96**, 1533 (1996).

[4] T. Poeschel et al., *Biophys. J.* **85**, 3460 (2003).

[5] E. McKintosh et al., *J. Neurovirol* **9**, 183 (2003).

[6] E. Pechkova, C. Nicolini, *Proteomics and Nanocrystallography*, Kluwer Academic Publishers, New York, 2003.

[7] A. Gadomski et al., *Materials Science-Poland* **24**, 935 (2006).

[8] A. Gadomski et al., *Chem. Phys.* **310**, 153 (2005).

[9] H. Tanaka, Y. Nishikawa, *Phys. Rev. Lett.* **95**, 078103 (2005).

[10] A. Gadomski, *Phys. A* **373**, 43 (2007).

[11] A. Irback, C. Troein, *J. Biol. Phys.* **28**, 1 (2002).

[12] J.R. Banavar et al., *Phys. Rev. Lett.* **93**, 238101 (2004).

[13] P. Meakin, A.T. Skjeltorp, *Advances in Physics* **42**, 1 (1993).

[14] J. M. G. Vilar, J. M. Rubí, *Proc. Natl. Acad. Sci. USA* **98**, 11081 (2001).

[15] M. Doi, S.F. Edwards, *The theory of polymer dynamics*, Oxford University Publications 1986.

[16] A. Gadomski, *Phys. A* **274**, 325 (1999).

[17] A. Gadomski, *Ber. Bunsenges. Phys. Chem.* **100**, 134 (1996); A. Gadomski, *Chem. Phys. Lett.* **258**, 6 (1996); A. Gadomski, Vacuum **50**, 79 (1998).

[18] D. Reguera et al., *J. Phys. Chem. B* **109**, 21502 (2005).

[19] A. Gadomski et al., Springer's Lecture Notes in Applied Mathematics, in press.

[20] N. Go, *Annu. Rev. Biophys. Bioeng.* **12**, 183 (1983).

[21] N. Kruszewska, A. Gadomski, *Conference of the Condensed Matter Division*, Dy 46.83, Dresden, Germany (2006).

[22] A. Gadomski, *Philos. Mag. Lett.* **70**, 335 (1994).

[23] H.D. Keith, F.J. Padden, *J. Appl. Phys.* **34**, 2409 (1963).

[24] N. Vandewalle, M. Ausloos, *Phys. Rev. E* **51**, 597 (1995).

[25] I. Santamaría-Holek, J.M. Rubi, *J. Chem. Phys.* **125**, 64907 (2006).

[26] K. Trojan et al., *Intern. J. Mod. Phys. C* **15**, 1121 (2004).

[27] T. Pöschel, T. Schwager, *Computational Granular Dynamics: Models and Algorithms*, Springer, Berlin 2005.

[28] I. Santamaría-Holek et al., *New J. Phys.* **7**, 35 (2005).

[29] G. Salvi, P. De Los Rios, *Phys. Rev. Lett.* **91**, 25 (2003).

[30] F. Scheffold et al., *Progress in Colloid & Polymer Science* **123**, 141 (2004); T. G. Mason et al., *J. Rheol.* **44**, 917 (2000).